DOI: 10.17725/j.rensit.2024.16.223

Designing a microchip for exosome isolation with the ability to simultaneously impregnate it with imatinib: an in vitro analysis

Amir Monfaredan, Elahe Motevaseli, Gholamreza Tavoosidana
Tehran University of Medical Sciences, Department of Molecular Medicine, School of Advanced Technologies in Medicine, http://en.tums.ac.ir/
Tehran 1416753955, Iran
E-mail: monfaredanamir@gmail.com, e_motevaseli@tums.ac.ir, g-tavoosi@tums.ac.ir

Fakher Rahim
Cihan University-Sulaimaniya, https://sulicihan.edu.krd/
Sulaimaniya 46001, Iraq
E-mail: rahim.fakher@sulicihan.edu.krd

Kudaiberdi G. Kozhobekov
Osh State University, https://oshsu.kg/
Osh 723500, Kyrgyzstan
E-mail: kudayberdi.kozhobekov@oshsu.kg

Mohammad Hossein Modarressi
Tehran University of Medical Sciences, Department of Medical Genetics, Faculty of Medicine, http://en.tums.ac.ir/
Tehran 1416753955, Iran
E-mail: modaresi@sina.tums.ac.ir

Alaviyehsadat Hosseininasab
GeneDia Life science company, https://tracxn.com/
Tehran 13000-15000, Iran
E-mail: shrzd.hsni@gmail.com

Ali-Akbar Aghajani-Afrouzi
Payame Noor University, Department of Business Administration, https://pnu.ac.ir/
Tehran 19569, Iran
E-mail: aghajaniali3@gmail.com

Mahdi Shafiee Sabet
Tehran University of Medical Sciences, School of Medicine, http://en.tums.ac.ir/
Tehran 1416753955, Iran
E-mail: mshafiees@sina.tums.ac.ir

Received January 17, 2024, peer-reviewed January 18, 2024, accepted January 19, 2024, published April 25, 2024

Abstract: **Exosomes, a small bilayer membrane derived from eukaryotic cells, have been identified as a useful natural delivery platform due to their suitable size, biocompatibility, structural stability, high loading capacity, and editable surface capability. Due to the difficulty of maintaining the highly pure exosome, several attempts have conducted the techniques for exosome isolation. In recent years, microstructures have found many applications in chemistry, biology, and medicine due to their high accuracy and low cost of materials. Soft lithography is a low-cost, fast, accurate, and yet widely used method of construction of Micron channels. In the present study, a soft lithography process has been performed to construct channels for exosome separation with immunoaffinity function. Both biochemical and biophysical categories tests were performed to examine the quality of extracted exosomes from different sources (serum, cell supernatant, and urine) and compared with the commercially available kit. Results showed that the current technique was capable to isolate exosomes with a high yield rate, purity, and low time consumption. All forms of the imatinib loaded exosomes exhibited the antitumor activity against KYO-1 cell line.**

Keywords: **personalized medicine; exosome; laboratory on a chip; leukemia; targeted therapy**

UDC 61:53(075.9)

Acknowledgements: This study was carried out in the form of a project approved under the number 99314850605 of the Faculty of Modern Medical Technologies of Tehran University of Medical Sciences. This study was supported by the Tehran University of medical sciences [grant no. 99-3-148-50605].

Ethics approval and consent to participate: This study was approved by ethics code number IR.TUMS. MEDICINE.REC.1399.969 in the Ethics Committee of the Faculty of Medicine of Tehran University of Medical Sciences

Authors' contributions: Amir Monfaredan analyzed data. Amir Monfaredan wrote the manuscript. Amir Monfaredan and Elahe Motevaseli contributed to the study concept, and drafted and revised the manuscript. Amir Monfaredan and Elahe Motevaseli confirm the authenticity of all the raw data. All authors read and approved the final version of the manuscript.

For citation: Amir Monfaredan, Fakher Rahim, Kudaiberdi G. Kozhobekov, Gholamreza Tavoosidana, Mohammad Hossein Modarressi, Alaviyehsadat Hosseininasab, Ali-Akbar Aghajani-Afrouzi, Mahdi Shafiee Sabet, Elahe Motevaseli. Designing a microchip for exosome isolation with the ability to simultaneously impregnate it with imatinib: an in vitro analysis. *RENSIT: Radioelectronics. Nanosystems. Information Technologies,* 2024, 16(2):223-238e. DOI: 10.17725/j.rensit.2024.16.223.

Contents

1. INTRODUCTION

Extracellular vehicles (EVs) or exosomes have developed as one of the interest fields due to their noteworthy role in not only biological processes but also, provide biocompatible vehicles for diagnosis and therapy [1]. Exosomes are small size biocompatible vesicles that are able to escape from mononuclear phagocyte system (MPS) [1]. The application of exosomes in biomedical diagnostics and therapy has highlighted the urgent need for new technologies in rapid and accurate methods of exosome separation in body fluids. Due to the biomolecule content of exosomes like proteins, nucleic acids (m. RNAs, microRNAs, and DNA), numerous attempts have conducted with the diagnostic and therapeutic potential of exosomes, related to their role in cell-cell communications and drug delivery, respectively. One of the main challenges is related to overcoming the fluid complexity and the lack of efficient techniques for isolation [2-4]. Exosomes are cell-derived structures packaged with lipids, proteins, and nucleic acids. They are found in various body fluids and play a role in physiological and pathological processes. Although their potential for clinical application as diagnostic and therapeutic tools has emerged, a major bottleneck hindering the development of applications in the rapidly growing field of exosome research is the inability to effectively separate purified exosomes from other undesirable components in body fluids. To date, various approaches for the isolation of exosomes have been proposed and investigated; their main candidate is

microfluidic technology due to its relative simplicity, cost-effectiveness, and ability for precise and rapid microscale processing and automation. In particular, eliminating the need for exosome labeling represents a significant advance in terms of process simplicity, time and cost, as well as in terms of preserving the biological activities of exosomes. Despite the exciting progress in microfluidic strategies for exosome isolation and the numerous advantages of label-free approaches for clinical applications, existing microfluidic platforms for exosome isolation still face a number of issues and challenges that hinder their use for sample processing [5-8]. This review focuses on recently developed microfluidic platforms for label-free isolation of exosomes, including those based on sieving, deterministic lateral displacement, field flow, and compressive flow fractionation, as well as viscoelastic, acoustic, inertial, electrical, and centrifugal forces [9-11].

In recent years, the field of microfluidics has made it possible to develop new methods for purifying exosomes. Microfluidics provides platforms, including micron-sized channels, for processing small amounts of fluids (microliters to picoliters). Most microfluidic devices are made with a special polymer called poly dimethylsiloxane) or PDMS [3,12,13]. PDMS is optically transparent and biocompatible, making them a useful material in constructing biofluid devices. Microfluidic platforms can classify exosomes with a high degree of purity and sensitivity while reducing the cost, time, and volume of reagents. The immunoaffinity-based microfluidic technique for exosome isolation overcomes many problems of traditional ones (such as ultracentrifugation, density gradient centrifugation, tangential flow filtration, size-exclusion chromatography) because they are adjustable, automatic, scalable, and portable. Exosomes can be isolated from other components of the sample based on the same specific proteins. CD9, CD41, CD63, and CD81as well as specific molecules like heparin, Tim4, and heat shock protein-binding peptides are common exosome surface markers for immunoaffinity-based isolation [14-17].

Herein, we have developed microfluidic devices for exosome isolation from different sources using CD68 conjugated magnetic beads [4,18,19].

2. MATERIALS AND METHODS

COMSOL simulations. The equations governing the channels were performed using COMSOL version 5.1 multiphysics software. The flow was simulated as a single-phase laminar flow and due to its thinness, the physical properties of distilled water at room temperature and pH = 7.4 were used for the simulation. The effective and optimized parameters were set as follows: The arrangement angle of the positions along the length of the chip, the designed curved channel width, the chip height, the number of mazes, the radius of curvature of the curved channel is designed, channel width at output and input, and Input flow rate.

Chip construction. Fabrication of exosome isolation microchip with the ability to load imatinib was done by standard soft lithography protocol. The silicon wafer was coated using SU8 photoresist (Microchem. Corp., Newton, MA). 5 cc of SU8 photoresist was poured on a 4-inch wafer and spin coating was done at 2300 rpm. Wafer baking after spin coat was done at 60 and 95 degrees Celsius for 2 hours and 15 minutes, respectively. After the baking was

completed, the mask was precisely aligned and exposed to UV light at 360 mV for 12 minutes on the wafer coated with SU8. After finishing the exposure, washing with developer and isopropanol was done for 4 minutes and 8 minutes, respectively, until the channels appeared. After preparing the mold, a 1:10 ratio of Polydimethylsiloxane (PDMS) (Microchem. Corp., Newton, MA) and hardener was prepared and bubbled. 10 cc of PDMS and hardener solution was poured on the mold and incubated at room temperature for 24 hours to form the PDMS chip. After the complete formation of the PDMS gel, using plasma gas with a power of 12 mJ/min for 4 minutes, stimulation was performed on the gel and the PDMS chip was attached to the glass (**Fig. 1**).

AFM microscopy. The topography, surface roughness, phase image, friction image, magnetic properties, and thickness of the monolayer is analyzed using AFM microscopy. To investigate the changes in chip level and post and channel heights, the chip was washed with acetone and dried at 60°C.

Microfluidic-based exosome extraction. The three primary exosomal sources including serum, urine, and cell culture supernatant were considered for this part of the study. Anti-CD63 (Abcam, UK) were conjugated to Mag nanoparticles (Jiayuan Quantum Pickup Company, Wuhan, China) using conventional methods. The total binding capacity of the nanoparticles was estimated to be about 10 μg of CD63 antibody on 1 mg of nanoparticles when using 1 mg/mL of Mag-CD63. The sample containing the exosome was mixed with CD63-Mag and inserted into the microfluidic chip via input 1, and the anti-CD63 (Abcam, UK) was re-inserted through input 2. A dual syringe pump with a flow rate of 1-10 μL/min flows were mixed in the first channel, resulting in the formation of the Mag-CD63-Exo complex. Immunomagnetic particles (CD63-Mag) were retained in chamber 1 by a magnetic disk. The PBS buffer was then introduced from input 3 to wash the Exo-CD63-Mag complex. It was then kept in compartment 2. Immuno-conjugate exosomes were collected for examination. The isolated exosomes from serum, urine, and cellular supernatant using a chip designed r named as S-EXOChip, UE-EXOChip, and SU-EXOChip, respectively. Also, the input 4 gate is defined for drug loading, which will be discussed further (**Fig. 2**).

Exosomes protein content. Bradford method was used to determine the protein content of the exosomes using 0.10, 0.08, 0.06, 0.04, 0.02 mg/mL of bovine serum albumin

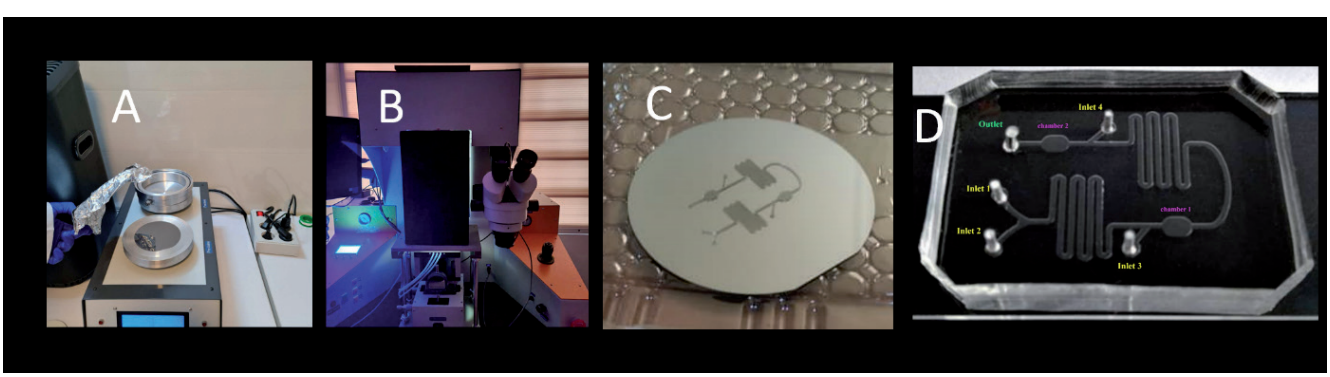

Fig. 1. *A: the steps of baking the wafer at temperatures of 60 and 95 degrees Celsius, B: the exposure process on the lined mask on the wafer, C: the final mold after the impact of the developer and washing with isopropanol, and D the final mold of the PDMS chip.*

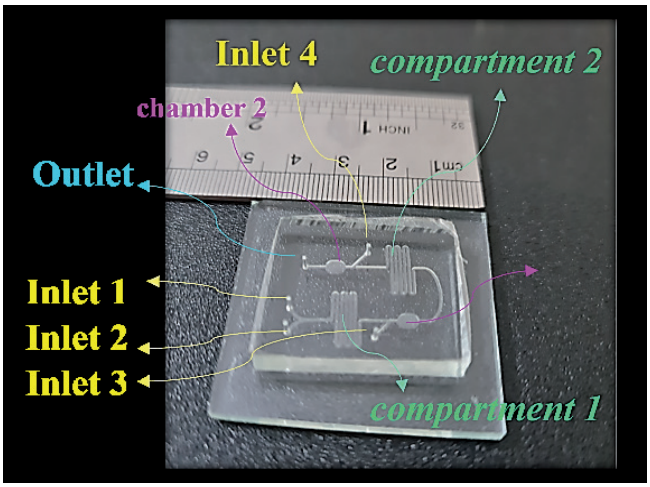

Fig. 2. *The variety of inputs, chambers, channels and output of the chip. In summary, entrance 1 and 2 are the place of injection of suspension containing exosome and specific magnet, entrance 3 is the entrance of PBS, chamber 1, the place where mixing is stopped by that trap, and entrance 4 is the place of imatinib loading.*

(BSA, Sigma, CAS no., 9048-46-8) at 595 nm [20].

Flow cytometry analysis. To evaluate the accuracy of the exosome extraction, flow cytometric analysis was performed against anti-CD63 antibody (Padza Padtenpajooh, cat#MM108, Iran) was performed on the extracted samples according to the manufacturer protocols. Briefly, 5 mg per test was added to the tubes containing exosomes, then tubes were gently mixed and incubated in the dark for 60 minutes at 2-8°C. After that, Wash the samples using 1 mL of diluted assay buffer 1X. To collect the magnetic grains, microtubes were placed in a magnetic circuit and then centrifuge at or at 3500×rpm for 10 min. Once more, 350 µL of assay buffer 1X is added to the tube and analyzed with flow cytometer (Millipore Merck Germany).

Exosome size and morphology analysis. For measuring the hydrodynamic size with DLS analysis, 200 µL of the exosomal solution of extracted cell supernatant was diluted with 420 µL of filtered PBS. The sample was then placed on ice and sonicated for 10 minutes. Finally, the sample was placed in a DLS device with 632 nm laser light beam and the results were analyzed with Zeta Sizer software.

Scanning electron microscopy (SEM) was used to analyze the size and morphology of the exosomes. Exosomes were coated with FEI Nova 200 Nanolab Dual-beam FIB scanning electron microscope under low energy (2.0-5.0 kV) in the Electron Microscopy Analysis Laboratory (MC2) by gold spraying or carbon by thermal evaporation. Then, 200 µL of extracted cell supernatant exosomes were poured onto the slide and dried for one hour at room temperature. The sample was then observed by electron microscopy.

Western blotting. The volume of 50 µL of lysis buffer was added to both extracted samples with a 1% Holt protease inhibitor (Thermofisher scientific, LTD, USA) and incubated for 2 min at room temperature. Then, samples were kept on ice for 10 minutes and centrifuged at 13000×rpm for 15 min at 4°C. finally, the samples were stored at –80°C for further analysis. The total volume of 20 µL of each sample was analyzed with 12% SDS polyacrylamide gel (SDWS-PAGE) is used to separate and determine the molecular weight of proteins with a voltage intensity of 80 mV. After separating the protein bands of the sample on SDS-PAGE gel, CD81 as a surface membrane-specific exosome protein was detected in cell lysate. In order to form an immunoblot cassette and load the gel and nitrocellulose paper on the blotting instrument (Biorad, USA). The transfer of protein bands was done for 90 min at a voltage of 100 mV. Afterward, the membrane was washed in the blocking buffer for 60 min at 37°C. Finally, the samples were stained with Anti-CD81 antibodies (1:4000) in TBS buffer (1x),

poured on PVDF membrane, and placed in a shaker incubator for 37 h at 37°C. Then it was washed three times with TBS buffer and each time for 10 min.

Exosomal RNA extraction and miRNA expression levels. RNA extraction was performed using Norgen's Exosome RNA Isolation Kit (Cat# 58000) according to the manufacturer's protocols. Initially, 300 μL of lysis buffer A and 37.5 μL of lysis buffer additive to each isolated exosome sample then, samples were mixed via vortexing for 10 seconds. After incubating the samples at room temperature for 10 min, 500 μL of 96% ethanol was added to the mixture and mixed well with Vertex for 10 seconds. Afterward, 500 μL of the mixture is transferred to the Mini Spin column and centrifuge at 6000×rpm for 1 min. After repeating the former step, 600 μL of washing solution A is added onto the column and centrifuge at 13000×rpm for 30 sec, followed by centrifuge at 13000×rpm for 1 minute. Finally, the volume of 50 μl of wash solution A is added onto the column and centrifuge at 8000×rpm for 1 min and stored at –80°C for further analysis.

The total non-coding RNAs and small RNAs such as miRNAs were converted to the cDNA extraction kit (ABM good Cat# G902). The miRNA sample was prepared by mixing 2 μL of 5X poly (A) polymerase reaction buffer, 1.5 μL ATP (10Mm), μmL $MnCl_2$ (25 mM), 0.5 μL Poly (A) Polymerase, Yeast (1μg/μL), and 2.5 μL of H_2O. Then, the mixture was incubated for 30 min at 37°C. Then 2 μl of miRNA Oligo (dT) adapter (10 mM) was added to the rest of the material. The mixture was incubated for 5 minutes at 65°C followed by cooling on crushed ice. Finally, 1 μL of dNTPs (10 mM), 4 μL of 5X RT buffer, 1 μl RTase (200U/ μL) and 2 μL H_2O were added to the above mixture. The cDNA synthesis was performed by incubating the samples for 15 min at 42°C and 10 min at 70°C. The microRNA content of the samples from three sources: urine, serum, and cellular supernatant was determined using the miRCURY™ LNATM microRNA Array Hy3™/Hy5™ kit (Exiqon, Denmark) following the standard protocols. Exosome isolation using Norgen Exosome Isolation Kit (Cat#58000) from three sources: urine, serum, and cellular supernatant. The qRT-PCR was performed for each sample in three Real-time PCR System by following the manufacturer's instructions and using different primers (**Table 1**). The mixture of 7 μL of Exiqon PCR Mastermix, 0.5 μL of panel Primer (5 pmol/μL), 3 μL of Tailed cDNA and 3 μL of Enhancer, and 4 μL of DEPC Treated water were prepared. The relative expression of miRNA-155 has assessed the method with U6 as a housekeeping control.

Drug loading. The modified method of direct incubation of the drugs and CD63-Mag captured exosomes with a freeze-thaw cycle to increase is used for loading imatinib. The exosomes were incubated with the imatinib with different concentrations. 10 nM of imatinib with an injection flow rate of 1μL/min was transferred to the input 4 of chips, at 25°C for 20 min. Then, papain and trypsin with concentrations of 0.1 and

Table 1

The qRT-PCR primers used for cDNA synthesis

Primers	Sequences
Mir150-5p-Forward	5'-TCCCAACCCTTGTACCAGTGAA-3'
Mir150-5p-Reverse	Universal
Mir92a-3p-Forward	5'-CACTTGTCCCGGCCTGTAA-3'
Mir92a-3p-Reverse	Universal
Mir155-5p-Forward	5'-TGCTAATCGTGATAGGGGTAAA-3'
Mir155-5p-Reverse	Universal
Mir378-Forward	5'-CTGGACTTGGAGGCAGAAAA-3'
Mir378-Reverse	Universal

0.02% have injected into the channel with a flow rate of 1 µL/min, respectively.

Drug release. The imatinib release was studied using a dialysis bag. 3 µg of exosome was homogenized in 3 mL of PBS buffer and then transferred to the dialysis bag and placed in a closed container with 60 mL of PBS buffer pH=7.4 and the temperature was stabilized at 37 °C. The released imatinib content was calculated and at the wavelength of 242 nm using UV-Visible spectroscopy. The standard curve was draw using 1, 2, 5, 10, 15, 20, and 25.30 µg/mL in PBS solution.

Cell toxicity. MTT assay is used to evaluate the toxicity of imatinib-loaded CD63-Mag captured exosomes against the KYO-1 cell line. The cellular metabolism of the cells was determined via monitoring the mitochondrial dehydrogenase enzymes activity using methylthiazole tetrazolium bromide (MTT) as a substrate. In this regard, 10,000 cells were pre-cultured in 96 well plates were incubated for 24 h at 37°C with 4% CO_2 and 90% humidity. The exosomal samples were with different concentrations including 2, 4, 8, 10, 20, 50, 100 mg/ml were treated for 24, 48, and 72 hours. Afterward, 20 µL of MTT solution (10 mg/mL) was added to each well and incubated for 4 h in the above-mentioned condition. Finally, the supernatant was discarded and 100 µL of DMSO was added to each well, shaken for 8 minutes in a circular motion, and then the absorption of formazan at 490 nm was measured using an ELISA reader. The cell viability percentage (IC50) was examined using Graphpad Prism 6.0 software (USA).

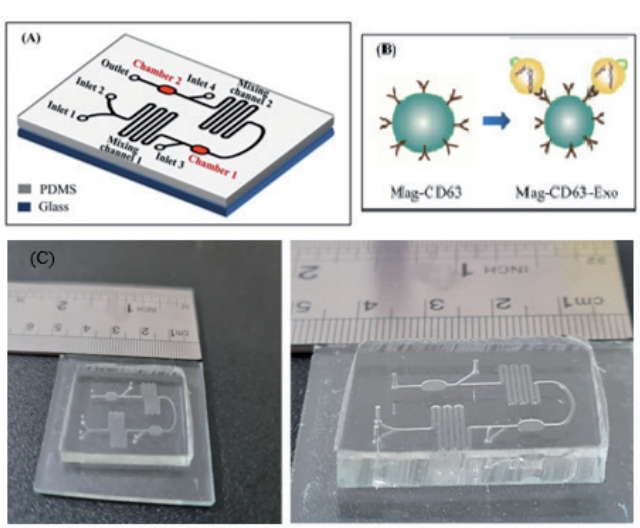

Fig. 3. *The schematic illustration of (A) and (C) microfluidic chip and (B) the principles of immunoaffinity-based exosome separation.*

Statistical Analysis. The statistical data was analyzed by Prism 7.0 (GraphPad Software, USA). The significance of RNA quantities and qRT-PCR validation of miRNAs among exosomes was evaluated with one direct T-test. The $p < 0.05$ was considered to be statistically significant.

3. RESULTS

In the present study, we used a microfluidic system for capturing CD63 conjugated magnetic beads for highly efficient exosome separation. Polydimethylsiloxane (PDMS) chip mold is made of SU-8 100 patterned silicon wafer using standard soft lithography technique with immunoaffinity function (**Figs 1** and **3**). Fig. 2 shows the variety of inputs, chambers, channels and output of the chip.

Images from an atomic force microscope (AFM) showed the surface of the chip. As illustrated in **Fig. 4**, the two-dimensional (2D) and three-dimensional (3D) images of the SU-8 100 surface. After extraction of the exosomes with CD68-Mag, the physicochemical properties of the extracted exosomes were investigated using DLS, SEM, flow cytometry, Bradford, qRT-PCR, and western blotting analysis. In this regard, exosome samples were examined by flow cytometry in the presents and

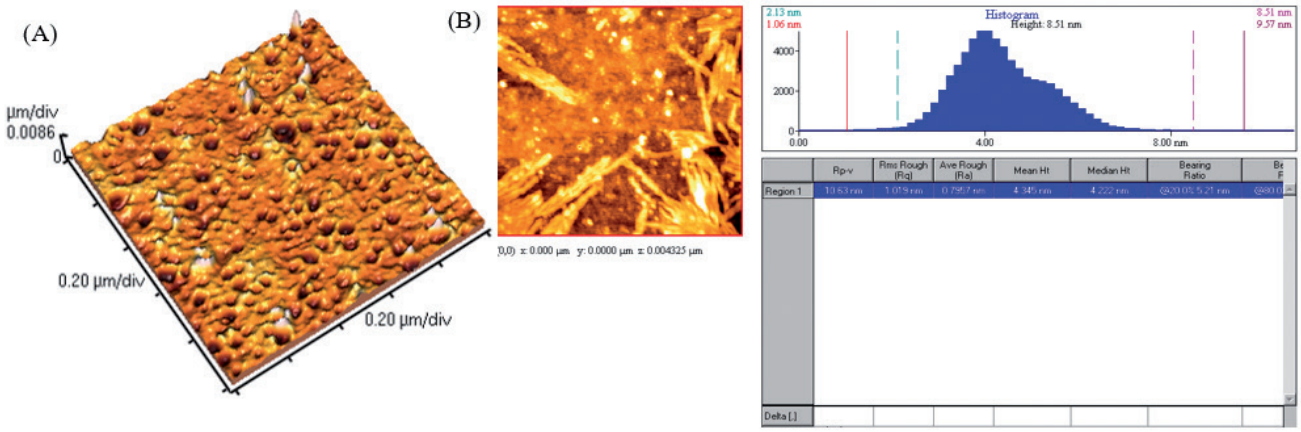

Fig. 4. *(A) 3D and (B) 2D images of the SU-8 100 chip surface.*

absence of protease enzyme (**Fig. 5***A-D*). The hydrodynamic size of the extracted exosome from various biological sources using both commercially available kit and SU-8 100 chip was evaluated. Fig. 5*E* showed the hydrodynamic size distribution of extracted exosomes via DLS analysis which estimated the majority population within the mean diameter of 135 nm. The SEM analysis image is shown in Fig. 5*F*. As it can be seen, spherical shape exosomes with a diameter between 30 and 175 nm could be detected. The Comparative study of cell supernatant and urinary derived exosome protein contents using chip and kit methods with semi-quantitative method Bradford is presented in **Fig. 6.** The protein content of serum and cellular supernatant were not significantly altered using both techniques. In the case of urinary extracted exosomes, although the commercially available protein content showed significantly higher, the proteins from the exosomes extracted by the chip are more homogeneous.

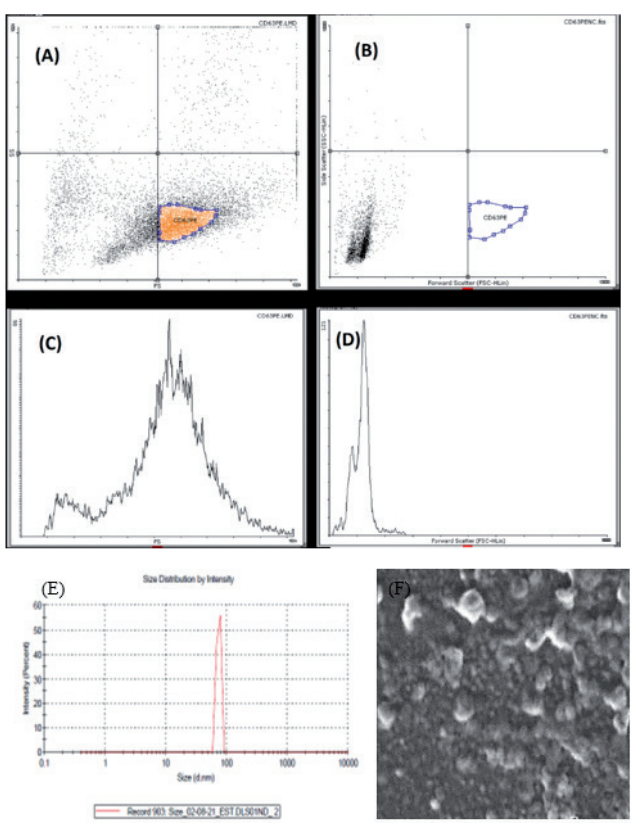

Fig. 5. *(A) The Flow cytometry analysis of the sample extracted by the chip against the CD68-PE antibody. (B) The chip extracted the sample in the presence of protease enzymes. (C) Chip-extracted sample histogram (D) Chip-extracted sample histogram in presents of protease enzymes. (E) The DLS histogram of isolates exosomes. (F) The SEM images of extracted exosomes.*

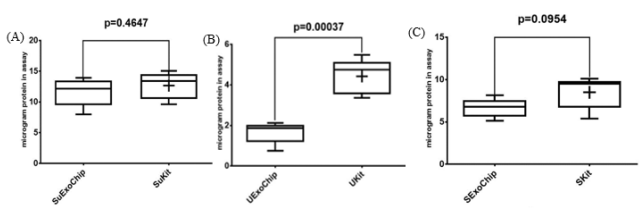

Fig. 6. *The protein content of the (A) cell supernatant, (B) urinary exosomes, and (C) serum using SU-8 100 chip commercially available kit with Bradford.*

Investigation of the expression profile of exosome microRNAs. After RNA extraction was performed under RNase free conditions, agarose gel electrophoresis was performed to confirm the health of RNAs and their quality. In gel examination, the presence of ribosomal S28, S18, and S5 bands indicates no RNA degradation. In addition, the smear observed between these two bands indicates the presence of mRNA (**Fig. 7***A*). The diagram below shows the y-axis showing microRNA expression based on its reference gene, U6, and the horizontal axis showing the origin of the exosome samples extracted by the commercialized kit and chip designed in this study. According to Figs 7*B* to 7*E* and

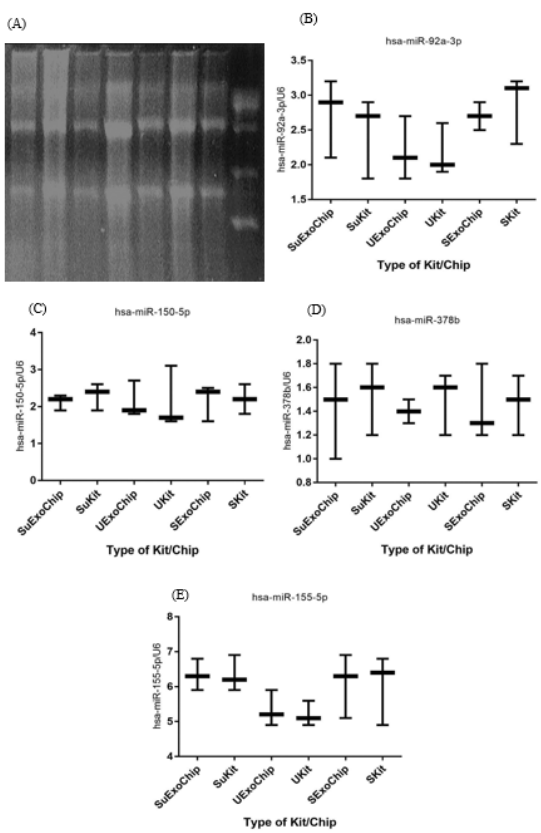

Fig. 7. *(A)The RNA extraction quality of exosome samples of serum, urine and cell supernatant using 2% agarose gel electrophoresis. The relative expression of (B) miR-92a-3p, (C) miR-150-5p, (D) miR-378, and (E) miR-155-5p in exosome samples of serum, urine, and cell supernatant using SU-8 100 chip and commercially available kit. The significance changes related to the RNA content of the experiment were analyzed using an unpaired t-test with a threshold of Pv < 0.05.*

Table 2

The statistical analysis of the expression fold samples of serum, urine, and cell supernatant using SU-8 100 chip and commercially available kit the significant pattern of miR-155 gene using non-paired T-test

	Fluid source	SU-8 100 chip	Commercially available kit	Values
miR-92a	Cell supernatant exosome	Fold Change		1.68
		p-value		0.6018
		T		0.5657
		df		4
		Significance		No
	Serum	Fold Change		1.39
		p-value		0.6164
		T		0.5423
		df		4
		Significance		No
	Urine	Fold Change		1.79
		p-value		0.9274
		T		0.09713
		df		4
		Significance		No
miR-150	Cell supernatant exosome	Fold Change		1.66
		p-value		0.5263
		T		0.6934
		df		4
		Significance		No
	Serum	Fold Change		1.96
		p-value		0.9319
		T		0.09091
		df		4

Table 2, no significant relative differences in miRNAs were observed. This indicates that the designed chip was able to isolate it without damaging the nucleic acid contents of the exosome.

The imatinib Release. Since the preservation of the drug carrier structure such as the exosome is very effective on drug release, the release of imatinib from the extracted exosomes was investigated using both imatinib-loaded CD63-Mag captured exosome with chip. Fig. 6*A* showed the adsorption peak taken from imatinib solution in PBS. As can be seen, imatinib maximum absorption peak is located at 242 ± 1 nm. The Calibration curve with R2 = 0.994 was

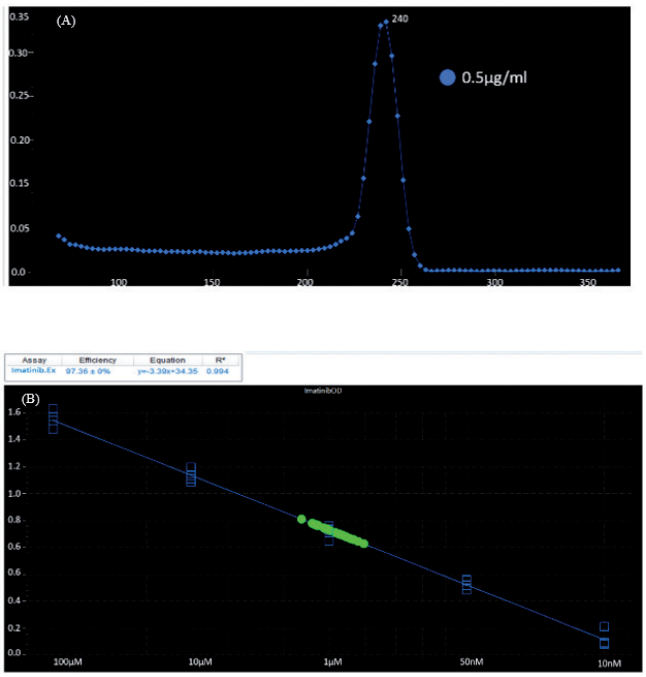

Fig. 8. *(A) The UV-Visible spectra of the imatinib-loaded CD63-Mag captured exosome with chip. (B) The linear equation of imatinib in PBS solution.*

presented to evaluate the drug release rate (**Fig. 8**).

Cell toxicity assessments. The comparison study of free imatinib, imatinib-loaded CD63-Mag captured exosome with chip and commercially available kit on the survival rate of KYO-1 cell line was done. According to **Figs 9***A* to 9*C*, the results indicate a dose-dependent toxicity of free imatinib, imatinib-loaded CD63-Mag captured exosome with chip and available kits on KYO-1 cells. In addition, when the cells were treated with the extracted exosome using a commercialized kit, the effective dose was changed to 100 µmol, but it is noteworthy that due to the preservation of the structure and morphology of the extracted exosome by the chip over time. The effective dose was equivalent to when imatinib was treated directly on the cells.

4. DISCUSSIONS

In the last decade, there has been a growing interest in the role of exosomes as the fluid

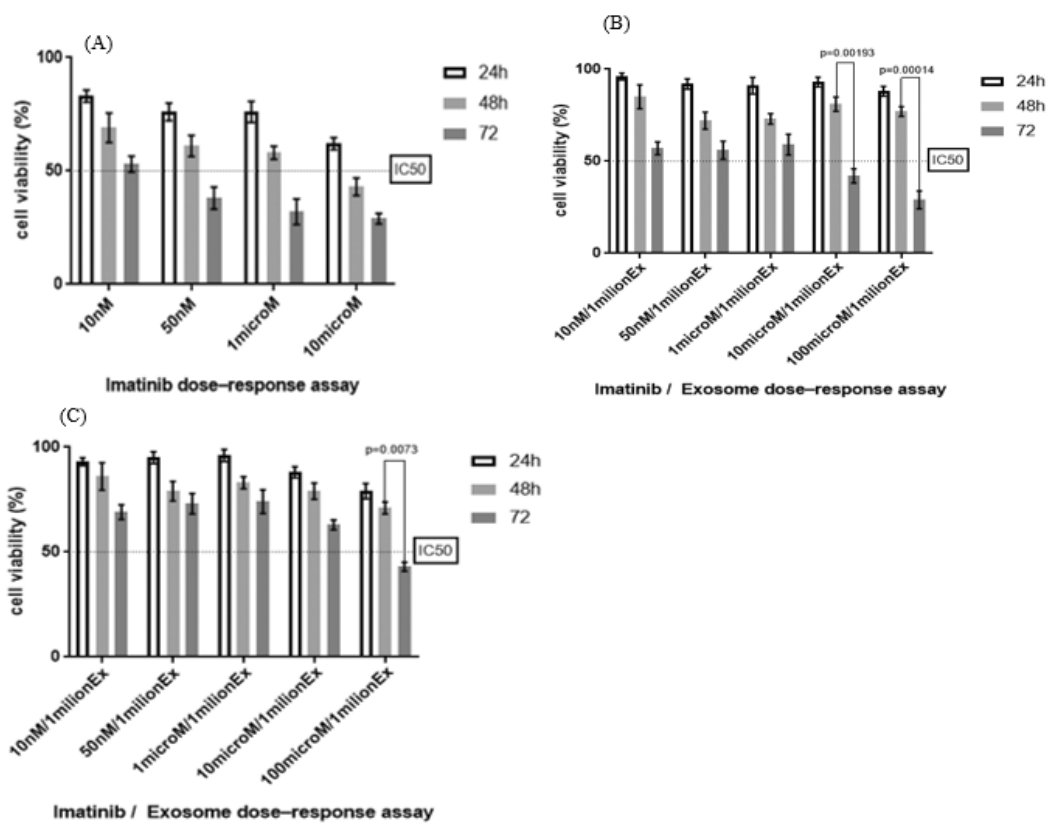

Fig. 9. *Cell viability at 24, 48 and 72 h of incubation by treating cells with (A) free imatinib, (B) imatinib-loaded CD63-Mag captured exosome with the chip, and (C) imatinib-loaded exosome using the commercially available kit.*

biopsy in the detection of cancer biomarkers. These studies have highlighted the urgent need for new technologies for the rapid and accurate separation of exosomes in body fluids with minimal sample preparation steps [21-25]. Exposure of exosomes to contamination and mechanical damage leads to serious issues in purity and more intact performance. The microfluidic-based exosome extraction improves the methods of many of the earlier techniques, in many aspects including isolation, molecular analysis, and detection. With the help of microfluidic technology, high-capacity exosome analyzes of up to 100 μL/min have been obtained with detection limits of about 50 exosomes/μL [3,26,27].

With the development of exosome research, it is recognized that exosomes are closely related to many physiological activities and the emergence and development of diseases. Therefore, exosome isolation and analysis are very important for exosome-related research and applications [14, 28-30]. However, traditional exosome isolation methods have many limitations, such as expensive instruments and reagents and significant time consumption. Compared with traditional methods, microfluidic technology has the advantages of high efficiency and high sensitivity in exosome separation. In recent years, with the rapid development of technology and more research, microfluidic technology has enabled the efficient separation, enrichment, and detection of multiple information of exosomes integrated into a single chip. This indicates that microfluidic chips have great potential in clinical research such as point-of-care testing [6,13,14,17,28-30].

Similar to this study has been conducted using anti-CD9 immuno-affinity magnetic beads using streptavidin –biotin conjugates on plasma samples with high separation efficiency and increased sensitivity. Also, bead-based protocols do not impose a limit on the sample size. In another study, anti-CD9 conjugated, anti-CD81, and antibody cocktail-conjugated magnetic nanowires magnetic beads were used for immunoaffinity isolation which provided approximately threefold greater yield than conventional methods. Also, Tim4 which binds specifically to the phosphatidylserine located on exosome cell surface, showed lower contamination than those obtained using conventional methods [31-33].

Microfluidic devices have been introduced to improve detection and isolation methods by facilitating the immunological separation, screening, and capture of exosomes. This makes them very attractive targets for disease detection and analysis. As a number of studies have shown, specific proteins and nucleic acids, the "cargo" of exosomes, can be an important source of biomarkers obtained from biofluids [34-37]. RNA analysis of exosomes from liquid biopsy samples could complement information from classical DNA analysis, clarifying specific processes and eventually paving the way for personalized medicine. Considering such aspects, liquid biopsy using microfluidic systems may also emerge as an important strategy in the development of personalized targeted therapy and disease monitoring [38]. The main scope of research into microfluidic devices will be how to overcome the challenges encountered on the path towards clinical translation and clinical application of exosomes as biomarker sources [39]. Various emerging microfluidic LOC platforms seek to increase the sensitivity of the isolation process and further facilitate in situ analysis. This is in line with the current trend and demand

for the realization of 'smart' systems with increased functionality and ease of use even by non-specialists in POCT [23]. Moreover, the realization, standardization and use of such advanced equipment could be the first step towards personalized healthcare. It may also bring closer the more distant goal of realizing a machine for the holistic separation and analysis of all liquid biopsy components to enable highly effective predictive medicine for truly personalized diagnosis and treatment [23]. To pave the way for such equipment to become widely accepted by medical practitioners worldwide, the complexity and difficulty of clinical trials and validation will also need to be overcome. Moreover, the ultimate challenge in the clinic is to perfect the technology, increase the dynamic range of the platforms, and produce cost-effective, specific, and sensitive devices for personalized medicine [4,8,17].

Particularly, immunoaffinity-based particle trapping is a highly specific way for exosome separation that can be integrated into microfluidic platforms. Several studies have conducted the use of antibody-conjugated magnetic beads for exosome separation. The CD9 conjugated magnetic beads in different sizes were tested for plasma exosome separation using an external force for magnetic beads movements with 10-15 times higher efficiencies than ultracentrifuges [27]. They have found that incubation of antibodies conjugated magnetic beads with solutions containing exosomes provided better conditions for the interaction between vesicles and ligands on the beads. In addition, bead-based protocols do not impose a limit on the sample size. Also, the microfluidic device based on immunoaffinity chromatography (CD63) was used for plasma exosomes from pancreatic cancer patients. The separation relies on receptors with additional input for adding lysis buffer for direct extraction of RNA and protein from the exosomes. Another approach for designing a microfluidic device was conducted using an input channel to label the exosomes with fluorescent dye to quantify the exosome on the chip. In this study, a microfluidic device was introduced as a platform for separating exosomes on the chip and a fluorescent assay for rapid quantification of exosomes. Other microfluids containing photo-lithography techniques based on micro-dimensional sites of graphene oxide (GO)/polydopamine (PDA) coated with protein G were investigated for ovarian cancer exosome separation. The designed system has potential to use the exosomes for diagnostic, and prognosis [27].

Chemotherapeutics can reduce tumor volume or cause short-term remission. However, cancer cells became resistant to chemotherapy over time. Drug resistance remains a barrier to achieving cure in patients with cancer. MSC-derived exosomes can be modified and applied in cancer therapy and promoting the chemosensitivity of cancer cells. For example, miR-302a from hucMSC exosomes suppressed cancer cell growth and migration. In another study, hucMSC-derived exosomes sensitized K562 cells to IM. Here, downregulation of miR-146a-5p in patients with CML, especially in patients with IM resistance, suggests an additional role in the acquisition of IM resistance. CML is a myeloid neoplasm caused by the BCR-ABL fusion gene, which causes dysregulated cellular proliferation and resistance to apoptosis through interference with downstream signaling pathways. It has recently been reported that miR-150 levels negatively correlate with BCR-ABL transcript

level and are significantly upregulated following reduction of BCR-ABL tyrosine kinase activity. The expression levels of miR-31, miR-155, and miR-564 were also reduced in CML and affected by BCR-ABL activity [7,40-42].

5. CONCLUSION

In summary, we developed a simple immunoaffinity-based microfluidic approach to for exosome separation by drug loading capacity. The designed system was capable to isolate exosome with high sensitivity, high recovery rate, and purity as well as low volume required and high-speed extraction procedure. The chip is scalable for the high-throughput isolation of exosomes with drug loading capacity for clinical uses. Hence, this platform should provide a useful tool in clinical applications for personalized medicine and as personal diagnostic devices in the future.

REFERENCES

1. Bernardi S, Farina M. Exosomes and Extracellular Vesicles in Myeloid Neoplasia: The Multiple and Complex Roles Played by These "Magic Bullets". *Biology* (Basel), 2021, 10(2).
2. Bernardi S, Foroni C, Zanaglio C, Re F, Polverelli N, Turra A, Morello E, Farina M, Cattina F, Gandolfi L et al. Feasibility of tumor-derived exosome enrichment in the onco-hematology leukemic model of chronic myeloid leukemia. *Int J Mol Med,* 2019, 44(6):2133-2144.
3. Gamage SST, Pahattuge TN, Wijerathne H, Childers K, Vaidyanathan S, Athapattu US, Zhang L, Zhao Z, Hupert ML, Muller RM et al. Microfluidic affinity selection of active SARS-CoV-2 virus particles. *Sci Adv,* 2022, 8(39):eabn9665.
4. Li Y, Cai T, Liu H, Liu J, Chen SY, Fan H. Exosome-shuttled miR-126 mediates ethanol-induced disruption of neural crest cell-placode cell interaction by targeting SDF1. *Toxicol Sci*, 2023, 195(2):184-201.
5. Jafarzadeh N, Gholampour MA, Alivand MR, Kavousi S, Arzi L, Rad F, Sadeghizadeh M, Pornour M. CML derived exosomes promote tumor favorable functional performance in T cells. *BMC Cancer,* 2021, 21(1):1002.
6. Kang KW, Jung JH, Hur W, Park J, Shin H, Choi B, Jeong H, Kim DS, Yu ES, Lee SR et al. The Potential of Exosomes Derived from Chronic Myelogenous Leukaemia Cells as a Biomarker. *Anticancer Res,* 2018, 38(7):3935-3942.
7. Keramati F, Jafarian A, Soltani A, Javandoost E, Mollaei M, Fallah P. Circulating miRNAs can serve as potential diagnostic biomarkers in chronic myelogenous leukemia patients. *Leuk Res Rep,* 2021, 16:100257.
8. Lan X, Yu R, Xu J, Jiang X. Exosomes from chondrocytes overexpressing miR-214-3p facilitate M2 macrophage polarization and angiogenesis to relieve Legg Calve-Perthes disease. *Cytokine,* 2023, 168:156233.
9. Li MY, Zhao C, Chen L, Yao FY, Zhong FM, Chen Y, Xu S, Jiang JY, Yang YL, Min QH et al. Quantitative Proteomic Analysis of Plasma Exosomes to Identify the Candidate Biomarker of Imatinib Resistance in Chronic Myeloid Leukemia Patients. *Front Oncol,* 2021, 11:779567.
10. Li P, Chen J, Chen Y, Song S, Huang X, Yang Y, Li Y, Tong Y, Xie Y, Li J et al. Construction of Exosome SORL1 Detection Platform Based on 3D Porous Microfluidic Chip and its Application in Early Diagnosis of Colorectal Cancer. *Small*, 2023, 19(20):e2207381.

11. Li Y, Xu M, Zhu Z, Xu F, Chen B. Transendothelial electrical resistance measurement by a microfluidic device for functional study of endothelial barriers in inflammatory bowel disease. *Front Bioeng Biotechnol,* 2023, 11:1236610.
12. Lu RXZ, Rafatian N, Zhao Y, Wagner KT, Beroncal EL, Li B, Lee C, Chen J, Churcher E, Vosoughi D et al. Heart-on-a-chip model of immune-induced cardiac dysfunction reveals the role of free mitochondrial DNA and therapeutic effects of endothelial exosomes. *bioRxiv,* 2023.
13. Pattabiraman PP, Feinstein V, Beit-Yannai E. Profiling the miRNA from Exosomes of Non-Pigmented Ciliary Epithelium-Derived Identifies Key Gene Targets Relevant to Primary Open-Angle Glaucoma. *Antioxidants* (Basel), 2023, 12(2).
14. Han Z, Peng X, Yang Y, Yi J, Zhao D, Bao Q, Long S, Yu SX, Xu XX, Liu B et al. Integrated microfluidic-SERS for exosome biomarker profiling and osteosarcoma diagnosis. *Biosens Bioelectron,* 2022, 217:114709.
15. Hu M, Brown V, Jackson JM, Wijerathne H, Pathak H, Koestler DC, Nissen E, Hupert ML, Muller R, Godwin AK et al. Assessing Breast Cancer Molecular Subtypes Using Extracellular Vesicles' mRNA. *Anal Chem,* 2023, 95(19):7665-7675.
16. Jafarzadeh N, Safari Z, Pornour M, Amirizadeh N, Forouzandeh Moghadam M, Sadeghizadeh M. Alteration of cellular and immune-related properties of bone marrow mesenchymal stem cells and macrophages by K562 chronic myeloid leukemia cell derived exosomes. *J Cell Physiol,* 2019, 234(4):3697-3710.
17. Lin S, Zhu B. Exosome-transmitted FOSL1 from cancer-associated fibroblasts drives colorectal cancer stemness and chemo-resistance through transcriptionally activating ITGB4. *Mol Cell Biochem,* 2023.
18. Mineo M, Garfield SH, Taverna S, Flugy A, De Leo G, Alessandro R, Kohn EC. Exosomes released by K562 chronic myeloid leukemia cells promote angiogenesis in a Src-dependent fashion. *Angiogenesis,* 2012, 15(1):33-45.
19. Wan Z, Chen X, Gao X, Dong Y, Zhao Y, Wei M, Fan W, Yang G, Liu L. Chronic myeloid leukemia-derived exosomes attenuate adipogenesis of adipose derived mesenchymal stem cells via transporting miR-92a-3p. *J Cell Physiol,* 2019, 234(11):21274-21283.
20. Ninfa AJ, Ballou DP, Benore M. *Fundamental laboratory approaches for biochemistry and biotechnology*. John Wiley & Sons, 2009.
21. Patterson SD, Copland M. The Bone Marrow Immune Microenvironment in CML: Treatment Responses, Treatment-Free Remission, and Therapeutic Vulnerabilities. *Curr Hematol Malig Rep,* 2023, 18(2):19-32.
22. Song F, Wang C, Wang C, Wang J, Wu Y, Wang Y, Liu H, Zhang Y, Han L. Multi-Phenotypic Exosome Secretion Profiling Microfluidic Platform for Exploring Single-Cell Heterogeneity. *Small Methods*, 2022, 6(9):e2200717.
23. Surappa S, Multani P, Parlatan U, Sinawang PD, Kaifi J, Akin D, Demirci U. Integrated "lab-on-a-chip" microfluidic systems for isolation, enrichment, and analysis of cancer biomarkers. *Lab Chip*, 2023, 23(13):2942-2958.
24. Taverna S, Amodeo V, Saieva L, Russo A, Giallombardo M, De Leo G, Alessandro R. Exosomal shuttling of miR-126 in endothelial cells modulates adhesive and

migratory abilities of chronic myelogenous leukemia cells. *Mol Cancer,* 2014, 13:169.

25. Wang QS, Xiao RJ, Peng J, Yu ZT, Fu JQ, Xia Y. Bone Marrow Mesenchymal Stem Cell-Derived Exosomal KLF4 Alleviated Ischemic Stroke Through Inhibiting N6-Methyladenosine Modification Level of Drp1 by Targeting lncRNA-ZFAS1. *Mol Neurobiol,* 2023, 60(7):3945-3962.
26. Corrado C, Raimondo S, Saieva L, Flugy AM, De Leo G, Alessandro R. Exosome-mediated crosstalk between chronic myelogenous leukemia cells and human bone marrow stromal cells triggers an interleukin 8-dependent survival of leukemia cells. *Cancer Lett*, 2014, 348(1-2):71-76.
27. Fonseca-Benitez A, Romero-Sanchez C, Lara SJP. A Rapid and Simple Method for Purification of Nucleic Acids on Porous Membranes: Simulation vs. Experiment. *Micromachines* (Basel), 2022, 13(12).
28. Giallongo C, Parrinello NL, La Cava P, Camiolo G, Romano A, Scalia M, Stagno F, Palumbo GA, Avola R, Li Volti G et al. Monocytic myeloid-derived suppressor cells as prognostic factor in chronic myeloid leukaemia patients treated with dasatinib. *J Cell Mol Med*, 2018, 22(2):1070-1080.
29. He L, Chen Y, Lin S, Shen R, Pan H, Zhou Y, Wang Y, Chen S, Ding J. Regulation of Hsa-miR-4639-5p expression and its potential role in the pathogenesis of Parkinson's disease. *Aging Cell*, 2023, 22(6):e13840.
30. Hrdinova T, Toman O, Dresler J, Klimentova J, Salovska B, Pajer P, Bartos O, Polivkova V, Linhartova J, Machova Polakova K et al. Exosomes released by imatinib-resistant K562 cells contain specific membrane markers, IFITM3, CD146 and CD36 and increase the survival of imatinib-sensitive cells in the presence of imatinib. *Int J Oncol,* 2021, 58(2):238-250.
31. Shi C, Pei S, Ding Y, Tao C, Zhu Y, Peng Y, Li W, Yi Y. Exosomes with overexpressed miR 147a suppress angiogenesis and infammatory injury in an experimental model of atopic dermatitis. *Sci Rep*, 2023, 13(1):8904.
32. Wang M, Zhang Z, Li G, Jing A. Room-Temperature Self-Healing Conductive Elastomers for Modular Assembly as a Microfluidic Electrochemical Biosensing Platform for the Detection of Colorectal Cancer Exosomes. *Micromachines* (Basel), 2023, 14(3).
33. Wang M, Zhao H, Chen W, Bie C, Yang J, Cai W, Wu C, Chen Y, Feng S, Shi Y et al. The SMAD2/miR-4256/HDAC5/p16(INK4a) signaling axis contributes to gastric cancer progression. *Oncol Res*, 2023, 31(4):515-541.
34. Yu H, Wu Y, Zhang B, Xiong M, Yi Y, Zhang Q, Wu M: Exosomes Derived from E2F1(-/-) Adipose-Derived Stem Cells Promote Skin Wound Healing via miR-130b-5p/TGFBR3 Axis. *Int J Nanomedicine*, 2023, 18:6275-6292.
35. Yu Z, Tang H, Chen S, Xie Y, Shi L, Xia S, Jiang M, Li J, Chen D. Exosomal LOC85009 inhibits docetaxel resistance in lung adenocarcinoma through regulating ATG5-induced autophagy. *Drug Resist Updat*, 2023, 67:100915.
36. Zhang B, Sun C, Liu Y, Bai F, Tu T, Liu Q. Exosomal miR-27b-3p Derived from Hypoxic Cardiac Microvascular Endothelial Cells Alleviates Rat Myocardial Ischemia/Reperfusion Injury through Inhibiting Oxidative Stress-Induced Pyroptosis via Foxo1/GSDMD Signaling. *Oxid Med Cell Longev,* 2022, 2022:8215842.

37. Zhang X, Wang C, Huang C, Yang J, Wang J. Doxorubicin resistance in breast cancer xenografts and cell lines can be counterweighted by microRNA-140-3p, through PD-L1 suppression. *Histol Histopathol,* 2023, 38(10):1193-1204.
38. Zhong AN, Yin Y, Tang BJ, Chen L, Shen HW, Tan ZP, Li WQ, He Q, Sun B, Zhu Y et al. CircRNA Microarray Profiling Reveals hsa_circ_0058493 as a Novel Biomarker for Imatinib-Resistant CML. *Front Pharmacol*, 2021, 12:728916.
39. Wang Y, Wang S, Chen A, Wang R, Li L, Fang X. Efficient exosome subpopulation isolation and proteomic profiling using a Sub-ExoProfile chip towards cancer diagnosis and treatment. *Analyst*, 2022, 147(19):4237-4248.
40. Cetin Z, Ilker Saygili E, Yilmaz M. Crosstalk between CML cells with HUVECS and BMSCs through CML derived exosomes. *Front Biosci* (Landmark Ed), 2021, 26(3):444-467.
41. Chinnappan R, Ramadan Q, Zourob M. An integrated lab-on-a-chip platform for pre-concentration and detection of colorectal cancer exosomes using anti-CD63 aptamer as a recognition element. *Biosens Bioelectron,* 2023, 220:114856.
42. Edlinger L, Berger-Becvar A, Menzl I, Hoermann G, Greiner G, Grundschober E, Bago-Horvath Z, Al-Zoughbi W, Hoefler G, Brostjan C et al. Expansion of BCR/ABL1(+) cells requires PAK2 but not PAK1. *Br J Haematol,* 2017, 179(2):229-241.